JACC: BASIC TO TRANSLATIONAL SCIENCE VOL. 8, NO. 1, 2023

ORIGINAL RESEARCH - PRECLINICAL

1-Year Patency of Biorestorative Polymeric Coronary Artery Bypass Grafts in an Ovine Model

Masafumi Ono, MD,[a,b] Shigetaka Kageyama, MD,[b] Neil O'Leary, PhD,[b] Mohammed S. El-Kurdi, PhD,[c] Jochen Reinöhl, MD, MSc,[c] Eric Solien, BS,[d] Richard W. Bianco, BS,[e] Mirko Doss, MD, PhD,[f] Bart Meuris, MD, PhD,[g] Renu Virmani, MD,[h] Martijn Cox, PhD,[c] Yoshinobu Onuma, MD, PhD,[b] Patrick W. Serruys, MD, PhD[b,i]

VISUAL ABSTRACT

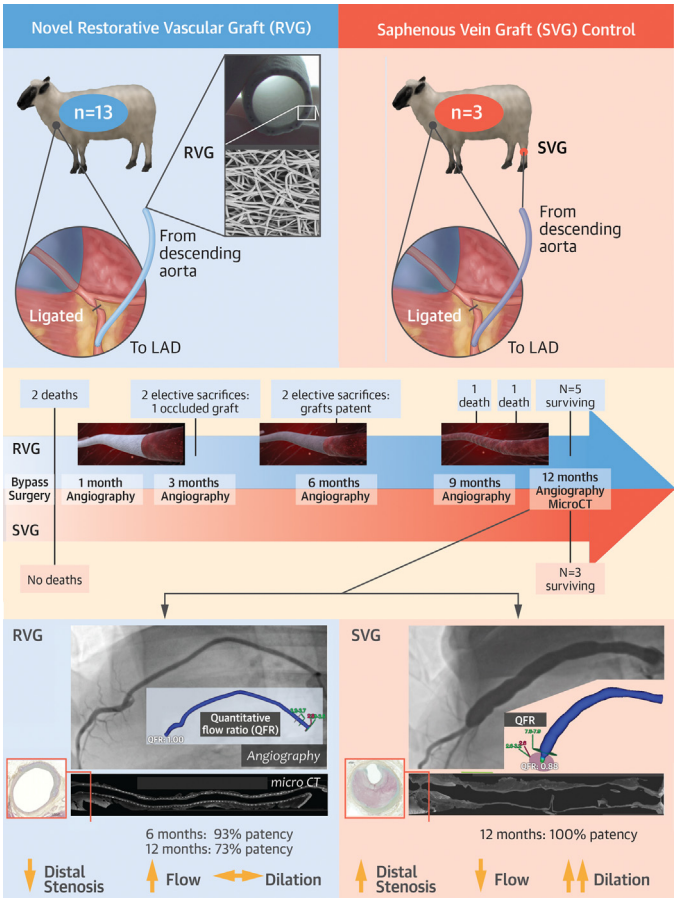

Ono M, et al. J Am Coll Cardiol Basic Trans Science. 2023;8(1):19-34.

HIGHLIGHTS

- **What are the feasibility and patency of a novel biorestorative polymeric graft implantation in animal models?**
- **The biorestorative grafts showed good patency out to 12 months, in a challenging ovine coronary artery bypass graft model. Saphenous vein graft showed progressive diffuse dilatation, while the reference diameter of biorestorative grafts remained stable.**
- **Serial angiography-based lumen and flow assessments in ovine models indicated the potential of this novel biorestorative bypass graft.**

From the [a]Amsterdam Universitair Medische Centra, University of Amsterdam, Heart Center, Department of Clinical and Experimental Cardiology, Amsterdam Cardiovascular Sciences, Amsterdam, the Netherlands; [b]Department of Cardiology, National University of Ireland, Galway (NUIG), Galway, Ireland; [c]Xeltis BV, Eindhoven, the Netherlands; [d]American Preclinical Services, LLC, Minneapolis, Minnesota, USA; [e]Experimental Surgical Services, University of Minnesota, Minneapolis, Minnesota, USA;

ISSN 2452-302X https://doi.org/10.1016/j.jacbts.2022.06.021

JACC: BASIC TO TRANSLATIONAL SCIENCE VOL. 8, NO. 1, 2023
JANUARY 2023:19–34

ABBREVIATIONS AND ACRONYMS

CABG = coronary artery bypass grafting

CPB = cardiopulmonary bypass

ePTFE = expanded polytetrafluoroethylene

IH = intimal hyperplasia

LAD = left anterior descending artery

OCT = optical coherence tomography

QCA = quantitative coronary angiography

QFR = quantitative flow ratio

RVG = restorative vascular graft

SVG = saphenous vein graft

SUMMARY

Many attempts have been made to inhibit or counteract saphenous vein graft (SVG) failure modes; however, only external support for SVGs has gained momentum in clinical utility. This study revealed the feasibility of implantation, and showed good patency out to 12 months of the novel biorestorative graft, in a challenging ovine coronary artery bypass graft model. This finding could trigger the first-in-man trial of using the novel material instead of SVG. We believe that, eventually, this novel biorestorative bypass graft can be one of the options for coronary artery bypass graft patients who have difficulty harvesting SVG.

Decades of development of alternative treatments for coronary revascularization, including angioplasty and stenting, suggest that complete coronary revascularization via coronary artery bypass grafting (CABG) using arterial grafts (left and right internal mammary arteries, radial artery, and/or gastroepiploic artery) provides the most durable solution.[1-3] However, autologous saphenous vein grafts (SVGs) are still used in the majority of CABGs because of their availability, the familiarity of use, and historical convention.[1] Because veins typically function in low-pressure hemodynamic conditions, arterial pressure can cause SVGs to distend and subsequently undergo dilation, yielding irregular lumen geometries. This action results in disturbances to hemodynamic factors that contribute to intimal hyperplasia (IH).[4-6] Reported SVG failure rates in CABG surgery are 10% to 30% at 1 year and ~50% at 10 years.[7-9]

Despite suboptimal performance, ~80% of all CABG surgery includes SVGs.[1,10] Many attempts have been made to inhibit or counteract SVG failure modes, including local delivery of genes[11] and drugs,[12] as well as improving the diameter and compliance mismatch at the anastomoses via external mechanical support.[1,13-17] However, to date, only external support for SVGs has gained momentum in clinical utility. The work by Taggart et al[1] has shown that by using external support to prevent dilation of SVGs, it was possible to reduce the rate of development of IH by attenuating hemodynamic disturbances caused by irregular lumen geometry. The impact of external stenting to SVG chronic performance in CABG has yet to be shown, and this will require long-term follow-up (~10 years) in a large population of patients.[18,19]

Harvesting of SVGs is associated with significant co-morbidity and poor quality of life due to the postoperative pain and distress felt by the patients in their legs at the harvest sites. Saphenous vein harvesting reportedly also causes severe scarring and additionally can lead to increased risk of infection due to poor wound healing in patients with poor peripheral circulation.[20,21] Although external stenting could improve the chronic durability of SVGs used in CABG, and thereby reduce the re-operation and/or re-intervention rates, the need to harvest the saphenous vein will remain.

An off-the-shelf, small-diameter vascular graft, that remains patent in the CABG circulation, could provide a valuable treatment alternative for millions of patients, annually. There are clinical reports of expanded polytetrafluoroethylene (ePTFE) grafts being used with some success in CABG,[22-26] but there are currently none approved for CABG use. This unmet clinical need persists because of the complex and elusive combination of polymer characteristics, material architecture, and surface modification needed to produce a graft that achieves chronic patency in CABG to match that of SVGs. All attempts to date have met with the same fate: inadequate thromboresistance with poor chronic patency. It is known that ePTFE grafts are rarely endothelialized >2 cm from each end, and this endothelial coverage is trans-anastomotically derived.[27] There is proof that a 4-mm inner diameter

[f]Department of Cardiac Surgery, Helios Clinic, Siegburg, Germany; [g]Department of Cardiac Surgery, University Hospital Leuven, Leuven, Belgium; [h]CVPath Institute, Inc, Gaithersburg, Maryland, USA; and the [i]NHLI, Imperial College London, London, United Kingdom.

The authors attest they are in compliance with human studies committees and animal welfare regulations of the authors' institutions and Food and Drug Administration guidelines, including patient consent where appropriate. For more information, visit the Author Center.

Manuscript received March 11, 2022; revised manuscript received June 29, 2022, accepted June 29, 2022.

FIGURE 1 **Illustration of Implant Configuration and Implant Angiography**

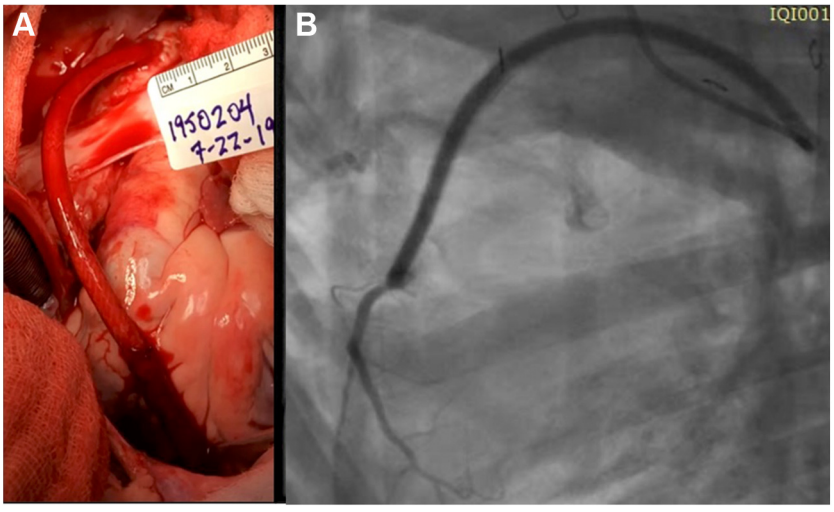

A total of 16 sheep were used in this study: 13 were implanted with a restorative vascular graft and 3 with a saphenous vein graft. Only 1 graft was implanted per animal.

ePTFE graft, with a preseeded autologous endothelium, achieved chronic patency in clinical CABG.[23] This finding illustrated that if a graft could naturally grow an endothelium in situ, then the thromboresistance problem could be overcome. The architecture of ePTFE (and other synthetic) grafts prevents the development of a confluent endothelium via transmural microvessel delivery of endothelial cells or transluminal seeding of endothelial progenitor cells.[27-30] Transmural microvessel connectivity between surrounding tissue and the graft lumen is needed to supply endothelial cells with sufficient density to form a confluent endothelium that is capable of providing chronic thromboresistance.

To create the necessary porous architecture for transmural and transluminal endothelialization, we proposed a restorative vascular graft (RVG), using electrospinning as the manufacturing method.[29] The polymer fiber morphology, interfiber bonding, and pore interconnectivity were controlled to promote microvessel growth through the wall to supply endothelial cells to populate the length of the graft with a confluent endothelium. Using a sheep CABG model, the present study evaluated the feasibility of implantation, and the evaluation of lumen geometry via serial angiographic assessment, of the RVG compared with an SVG control. The study was also intended to provide data to inform future development of this approach toward clinical use.

METHODS

ETHICS STATEMENT. Angiography data at baseline and follow-up were acquired from the animals implanted with the biorestorative bypass graft (Xeltis BV, Eindhoven, the Netherlands). The study was conducted in accordance with the Guide for Care and Use of Laboratory Animals and the ARRIVE guidelines (Animal Research: Reporting of In Vivo Experiments) and was approved by the Test Facility's Ethical Committee for compliance with regulations before study initiation (Protocols IQI001-IS02 and IQI005-IS02).

DEVICE MANUFACTURING. The 4-mm inner diameter, 500-μm wall thickness, 15-cm long grafts used in this study were constructed from 2 main components, the electrospun biorestorative polymer scaffold and an embedded nitinol micro skeleton. First, an inner electrospun layer was deposited onto a cylindrical target; the micro skeleton was then deployed over the inner layer, and then an outer electrospun layer was deposited over the micro skeleton, embedding it within the polymer scaffold. The distal 2-cm end of the graft does not have an embedded nitinol micro skeleton and was fully trimmable for creating the distal anastomosis. The proximal end of the graft has a series of 5 embedded nitinol rings, which provided some length trimmability for length adjustment and trajectory planning. The graft was trimmed close to

JACC: BASIC TO TRANSLATIONAL SCIENCE VOL. 8, NO. 1, 2023
JANUARY 2023:19–34

FIGURE 2 Image of RVG With Blow-Up to Show SEM Morphology

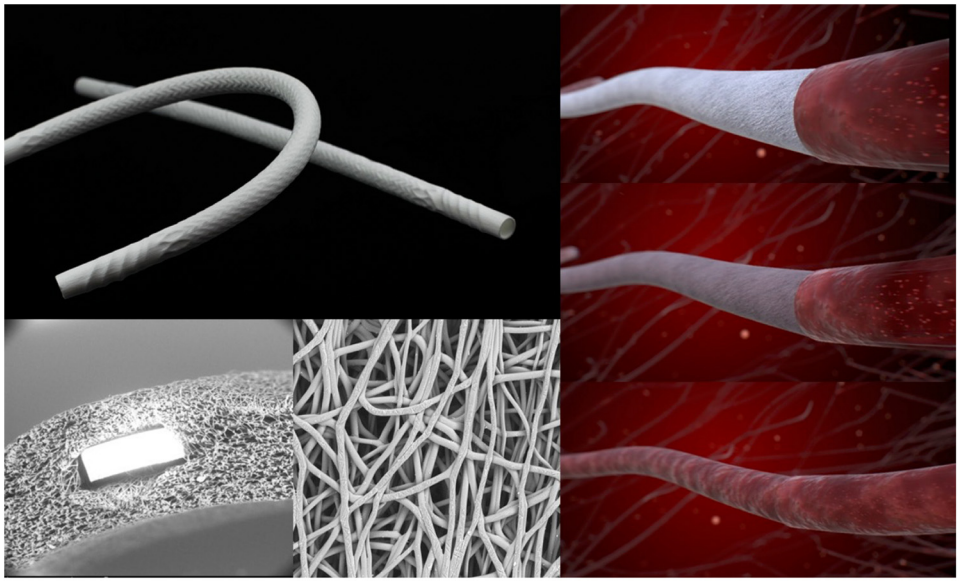

A representative photograph of a restorative vascular graft (RVG) is presented in the **left upper panel**. A representative scanning electron photomicrograph of the outer surface of a device is shown in the **lower left**. The device exhibits a highly porous morphology characterized by bonded overlapping fibers ~5 μm in diameter. RVG = restorative vascular graft; SEM = scanning electron microscopy.

one of the rings, and the ring was sewn into the proximal anastomosis.

ANIMAL STUDY DESIGN. A total of 16 sheep were used in this study: 13 were implanted with an RVG, and 3 were implanted with an SVG. Only 1 graft was implanted per animal as shown in Figure 1. All animals were given dual antiplatelet therapy of aspirin (325 mg on day -4, and 81 mg on day -3 and daily thereafter) and clopidogrel (150 mg on day -4, and 75 mg on day -3 and daily thereafter), in line with previous reports.[31] The sheep CABG model that was used in this study is based on the model used by Shofti et al.[30] Briefly, a left lateral thoracotomy was routinely performed, and the pericardium was opened and cradled. Graft placement was between the descending aorta and the left anterior descending coronary artery (LAD). Once heparin anticoagulation was initiated, and an activated clotting time of approximately 350 seconds was achieved (and maintained throughout the procedure), cannulas were placed, and cardiopulmonary bypass (CPB) was initiated. Cardiac arrest was induced via use of Plegisol (Pfizer) or del Nido (Nephron Pharmaceuticals) solutions, and additional cardioplegia solution was administered every 20 minutes as needed. The distal end of the RVG was trimmed and prepared for implantation. An arteriotomy was performed in the LAD artery, and the RVG was sewn in an end-to-side fashion to create the distal anastomosis. The graft was then retrograde flushed with blood and isotonic fluids to test patency and sealing of the suture line. To allow creation of the proximal anastomosis, a bulldog-type clamp with protective boots was applied to the distal portion of the graft. An aortotomy was made in the partially occluded descending aorta using a stab incision and a 4- to 6-mm aortic punch to create the proximal anastomosis site. The graft was trimmed and sewn into the anastomosis. Before completion of the proximal anastomosis, air was evacuated from the graft by releasing the bulldog-type clamp, and the proximal anastomosis suture was tied tight after all air had escaped. Blood flow was established in the graft, and any additional required repairs to the anastomoses were made. After graft implantation was completed, the LAD was ligated a few millimeters upstream of the graft distal anastomosis. The heart was defibrillated (if needed) to establish a sinus rhythm, and CPB was discontinued.

The RVGs were implanted after unpacking, as intended. The autologous saphenous veins required harvesting before implantation, as follows. A medial longitudinal skin incision was made between the hock and the stifle on 1 hind-limb. The saphenous vein was identified and isolated via dissection. Side

FIGURE 3 Study Flowchart

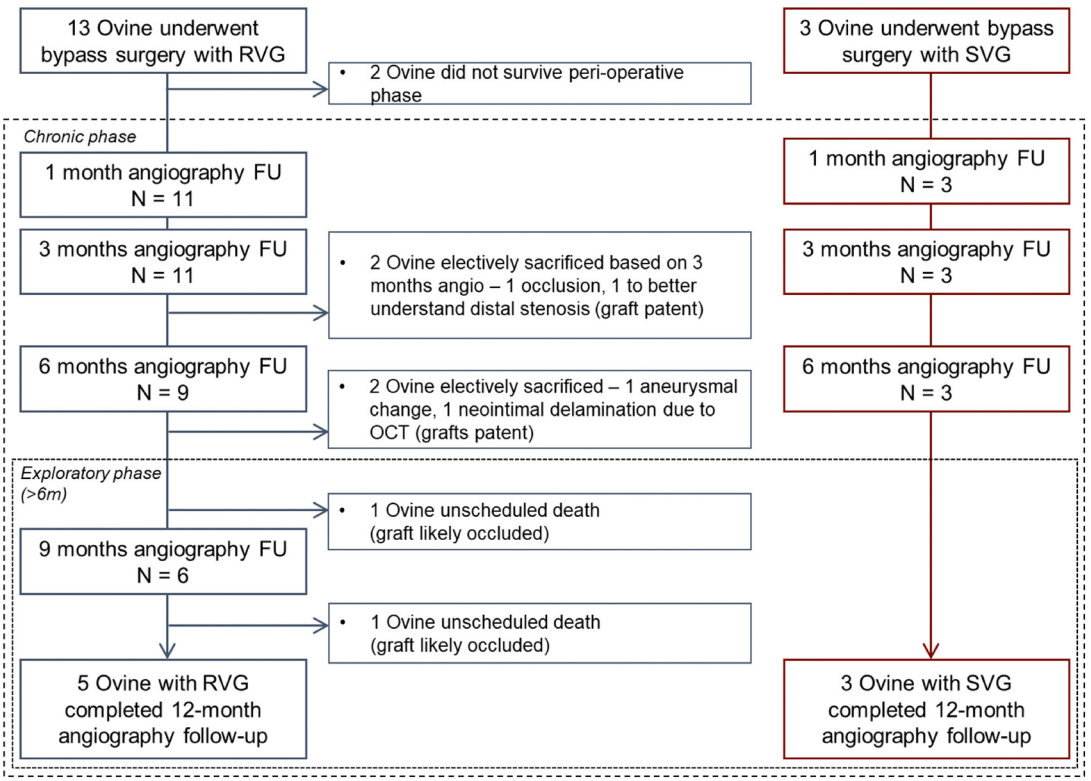

The study design and timeline are described in the schematic diagram. FU = follow-up; OCT = optical coherence tomography; RVG = restorative vascular graft; SVG = saphenous vein graft.

veins, if present, were ligated routinely by using 4-0 polyester suture. The distal aspect of the vein segment was ligated, and the proximal aspect of the vein segment was clamped. The SVG segment was cannulated at the proximal end of the graft segment (distal to clamp). The graft was then excised and placed in heparinized isotonic fluid until time of implantation. The SVGs were implanted by using an identical technique as for the RVGs. Wound closure and postoperative care were according to the standard of care.

Animals were initially intended to be euthanized after 6 months' survival, and the safety of the RVG was to be compared vs that of the SVG control. However, by 6 months, there were few complications and also very promising angiographic results. Thus, the advisory board recommended extending the study beyond 6 months in an exploratory effort to maximize the learnings from the study.

ANGIOGRAPHY IMAGING METHODS. Arterial blood pressure was recorded during all angiographic imaging to help ensure that dimension measurements were not affected by blood pressure. Each animal was administered a single dose of heparin (50 IU/kg) and had continuous monitoring of activated clotting time values. A reduced heparin administration approach was used to limit postprocedural hemorrhage.

A 5-F sheath and catheter were placed in the femoral artery, either via cut-down or percutaneously, for angiography. Either the right or left femoral artery was used. A diagnostic catheter (over a guidewire) was passed to the proximal aspect of the graft. The graft was intubated and contrast was injected to assess the graft and distal perfusion run-off. Selective bypass angiography from the ostium of the RVG was performed with a JR 4.0 catheter (Medtronic). The angiography was obtained in at least 2 orthogonal angiographic views (antero-posterior and left anterior oblique 90 °) to assess the graft ostium, the full graft body, and the distal anastomosis for quantitative coronary angiography (QCA). Sufficient run-off was documented. All filling defects present were also

FIGURE 4 Serial Angiography Snapshot Images of All RVGs and SVGs in Animals That Survived to the 12-Month Follow-Up

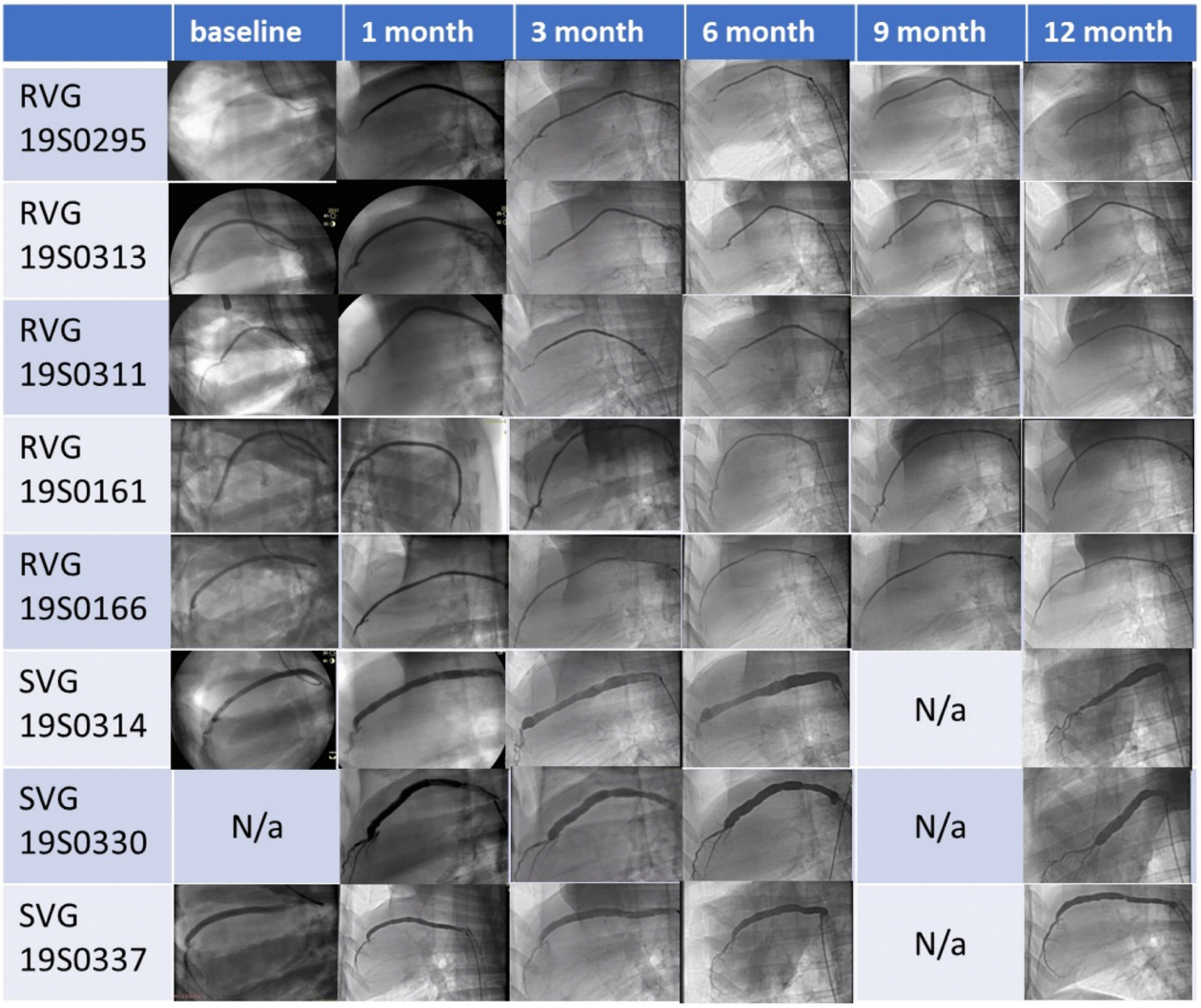

Representative snapshots from angiograms of all RVGs and SVGs in animals that survived to 12 months are presented. N/a = not applicable; other abbreviations as in Figure 3.

noted. All data acquisition parameters were documented to aid with subsequent analysis as described in the following sections.

ANGIOGRAPHIC ANALYSIS. QCA with edge detection (interpolated reference diameter, minimal lumen diameter, and diameter stenosis) and videodensitometry (minimal luminal area, reference area, and area stenosis), quantitative flow ratio (QFR), mean flow velocity, and volumetric flow (mean area × mean flow velocity) were analyzed by an independent core laboratory (CORRIB Corelab, National University of Ireland Galway).[32,33] In the QCA analysis, the reference diameter is determined according to the interpolated technique excluding the narrowed segments using an end-diastolic angiographic frame.

Aneurysmatic dilatation was defined as focal dilation of at least 1.5 times the adjacent normal segment.[34] Diffuse dilatation was defined when one-third of the whole graft length at follow-up exceeded the baseline (1-month) mean diameter of the SVG or the nominal diameter of the RVG by 50%.[35]

Mean blood velocity was assessed by using the Thrombolysis In Myocardial Infarction frame count.[36] The total number of frames was counted, from the initial complete opacification of the proximal anastomosis of the graft, to the frame where dye first

TABLE 1 Summary of Angiographic Parameters

		Reference Diameter (mm)						Minimal Lumen Diameter (mm)						Flow Speed (cm/s)						QFR					
	ID	B	1M	3M	6M	9M	12M	B	1M	3M	6M	9M	12M	B	1M	3M	6M	9M	12M	B	1M	3M	6M	9M	12M
RVG	19S0166	3.7	2.9	2.8	2.9	3.0	2.8	3.0	2.5	1.5	1.9	1.5	1.7	6.8	9.6	18.0	14.0	15.0	5.0	1.00	0.99	0.75	0.94	0.92	0.94
	19S0217	3.8	3.3	4.2				3.2	2.7	1.9				29.9	9.6	24.0				0.99	1.00	0.90			
	19S0161	3.4	3.7	3.4	3.5	3.3	3.0	3.0	2.5	1.6	2.3	2.2	1.9	11.5	7.7	23.0	23.0	21.0	14.0	0.97	0.96	0.56	0.94	0.97	0.83
	19S0204	3.6	3.8	N/a[a]				3.3	2.0	N/a[a]				17.8	6.8	N/a[a]				0.99	0.95	N/a[a]			
	19S0212	3.9	3.6	3.4	4.0			3.6	2.8	1.7	1.7			13.0	5.0	6.3	7.8			0.99	0.94	0.91	0.71		
	19S0295	3.6	3.3	3.2	3.3	2.7	3.7	2.8	2.8	2.5	2.6	1.9	2.8	7.7	8.2	19.0	10.0	14.0	20.0	N/a	N/a	0.94	0.99	0.96	0.99
	19S0313	4.3	3.7	3.0	3.6	2.8	3.4	3.3	3.0	2.6	2.9	2.7	2.9	9.3	11.0	8.8	9.7	12.0	14.0	0.99	N/a	1.00	0.99	1.00	1.00
	19S0311	3.6	3.6	3.7	3.7	3.2	3.5	2.8	2.3	1.9	2.0	1.8	2.0	12.1	7.0	11.0	14.0	28.0	17.0	0.99	0.98	0.79	0.80	0.71	0.87
	19S0328	3.7	3.6	3.9	3.7			3.6	3.0	2.2	2.2			20.6	6.6	7.0	18.0			1.00	1.00	0.75	0.78		
	19S0333	3.3	4.1	4.0	3.4			2.8	2.9	2.1	2.0			14.1	7.9	31.0	29.0			1.00	0.99	0.53	0.81		
	19S0329	N/a	3.9	3.9	3.2	2.7		N/a	2.8	2.6	1.6	1.4		N/a	15.0	14.0	23.0	19.0		N/a	0.99	0.69	0.53	0.46	
	Mean	**3.7**	**3.6**	**3.5**	**3.5**	**2.9**	**3.3**	**3.2**	**2.7**	**2.1**	**2.1**	**1.9**	**2.2**	**14.3**	**8.6**	**16.0**	**17.0**	**18.0**	**14.0**	**0.99**	**0.98**	**0.78**	**0.83**	**0.84**	**0.93**
	STD	0.3	0.3	0.5	0.3	0.2	0.4	0.3	0.3	0.4	0.4	0.5	0.5	7.0	2.7	8.2	7.2	5.8	5.6	0.01	0.02	0.16	0.14	0.19	0.07
SVG	19S0314	4.6	5.2	8.9	11.0		11.5	4.4	2.1	5.9	4.8		4.0	3.5	1.7	1.0	1.5		1.8	1.00	N/a	0.95	0.91		0.99
	19S0330	4.9	6.2	7.5	9.0		9.1	4.1	3.5	3.4	3.7		5.3	7.2	2.5	1.6	3.8		3.7	0.99	N/a	0.97	0.95		0.81
	19S0337	4.2	6.1	5.7	6.1		7.8	4.2	2.9	2.6	2.9		4.9	6.7	2.6	2.7	3.2		4.7	0.97	0.88	0.95	0.86		0.81
	Mean	**4.6**	**5.8**	**7.4**	**8.6**		**9.5**	**4.2**	**2.8**	**4.0**	**3.8**		**4.7**	**5.8**	**2.3**	**1.8**	**2.9**		**3.4**	**0.99**	**0.88**	**0.96**	**0.91**		**0.87**
	STD	0.3	0.6	1.6	2.3		1.9	0.2	0.7	1.7	0.9		0.7	2.0	0.5	0.9	1.2		1.5	0.02	N/a	0.01	0.05		0.10

[a]Graft occluded at 3-month angiographical follow-up; in the statistical analyses (Supplemental Tables 1 and 2), the quantitative coronary angiography (QCA) value of the occluded graft is included as 0 mm (% diameter stenosis is considered as 100%).

B = baseline; M = month follow-up; NA = not applicable; QFR = quantitative flow ratio; RVG = restorative vascular graft; SVG = saphenous vein graft.

enters the native coronary artery at the distal anastomosis. Then mean volumetric flow was calculated by multiplying the mean blood flow velocity by the reference lumen area of the graft.[37]

Offline QFR analysis was performed with the QAngio XA 3D software version 2.0 software package. The QFR calculation is based on the 3-dimensional QCA reconstructed from 2 angiographic projections separated by an angle ≥25 °(in the present case, 90 °), and flow velocity is computed from the contrast bolus frame count. In cases with only single analyzable projection, single-projection QFR based on bifurcation fractal law (μQFR) was used instead.[38] Although conventional edge and video densitometric QCA were analyzable in a single projection, QFR was not available in 3 grafts (2 RVG and 1 SVG) because the grafts had been filmed without isocenter calibration.[39] One SVG had a poor angiographic image quality (poorly selective injection) precluding precise contour delineation. In case of graft occlusion, QFR was considered as 0.

Vessel QFR was analyzed from the ostium of the bypass graft, through the anastomosis, up to the first distal anatomical landmark in the native vessel (eg, as a first side branch of the LAD, major or minor).

PATENCY EVALUATION. At each time point of angiography follow-up, patency of grafts was assessed as a binary condition. The grafts were evaluated as either patent or occluded. The aggregated patency rates were calculated for both RVGs and SVGs, at both 6 and 12 months, as the ratio of patent grafts to total number of grafts implanted, multiplied by 100%.

STATISTICS. In descriptive statistics, categorical variables were expressed as counts with percentages and continuous variables are presented as the mean ± SD or median with the 25th and 75th percentiles (quartile 1, quartile 3).

Given our aims to examine differences in each angiography-derived parameter between groups (RVG and SVG) and across 1-year of follow-up, we chose an approach that could provide inference on these factors simultaneously and which could use all available data in an imbalanced data structure that was reasonably robust to the occasional missing follow-up data in the study. Thus, we used a linear mixed effects model for each angiography-derived parameter with group (2-level factor) and time (5-level factor [1 level per follow-up assessment]) as the 2 fixed effects and animal as a random intercept. A likelihood ratio test of both factors for each parameter model provided the degree of evidence for a difference between groups or over time. A time-group interaction effect was also assessed by inclusion in models for parameters in which the main effects of time and group differences were found to be statistically significant.

Given the volume of parameters assessed, we also adjusted test inferences to control for a false-positive

rate within each family of hypotheses (group differences and differences across time) using the Holm-Bonferroni method.

Serial follow-up data were plotted for each parameter and separated by group with a locally estimated scatterplot smoothing curve fitted to characterize any changes over time and between groups.

All statistical tests were 2-tailed, and a *P* value of 0.05 was considered as statistically significant, after adjustment for multiple testing outlined earlier. Statistical analyses were performed by using R version 4.1.2 (R Foundation for Statistical Computing).

RESULTS

DEVICE CHARACTERIZATION. All devices were grossly free of defects (as assessed via unmagnified, corrected vision under illumination per ISO 7198,[40] such as the presence of holes and other discontinuities or imperfections of fabrication, and for the presence of dirt, soiled areas, spots, stains, or loose particles). A representative photograph of an RVG is presented in **Figure 2**, along with a representative scanning electron photomicrograph of the outer surface of a device. The device exhibits a highly porous morphology characterized by bonded overlapping fibers ~5 μm in diameter.

ANIMAL STUDIES. All animals (N = 16) were implanted successfully, except for a technical error in 1 animal, which resulted in the distal anastomosis being sewn closed. Angiography showed that the graft was occluded in this animal, and the anastomosis was not repairable, and thus the animal was euthanized. Another animal also did not survive the implantation procedure due to severe blood loss during the graft sealing step. The porosity of the experimental graft required it to be sealed with blood intraoperatively, which was typically completed just before weaning from CPB. However, assessment of this particular animal's baseline blood cell count showed that the animal had too few platelets to generate a reliable value, and graft sealing was not possible. The animal was euthanized and replaced with another backup animal.

Four RVG animals were euthanized early (before the final 12-month follow-up) to better understand angiographic observations. One animal had an occluded graft, and one animal showed a distal stenosis at the 3 months' follow-up angiogram. One animal had a nonruptured aneurysm in the body of a patent graft at the time of the 6-month follow-up angiogram (Supplemental Figure 1). Finally, optical coherence tomography (OCT) disclosed at 6 months in one animal a neointimal delamination, which was likely iatrogenic (either caused or aggravated by insertion of the OCT catheter) (Supplemental Figure 2). All 4 animals were euthanized to allow explant analysis of the grafts and to help determine the etiology of the angiographic and/or OCT observations.

All 3 SVG control animals were implanted successfully and survived to their intended termination time point of 1 year. The aggregated patency rate at 6 months was 90.9% (10 of 11) for the RVGs and 100% (3 of 3) for the SVG controls. Based on the encouraging results at 6 months with only few complications, the original endpoint of 6 months was extended in an exploratory effort to maximize learnings. Ultimately, 72.7% (8 of 11) of the implanted RVGs were patent when considering all surviving RVG animals in aggregate after 1 year of implantation. The study design and timeline are described in the schematic diagram in **Figure 3**.

QCA AND QFR ANALYSES. Qualitative angiographic assessment of all RVGs, which survived to the 12-month time point, revealed smooth and uniform luminal geometries throughout the study. In stark contrast, the SVGs displayed irregular and severely dilated geometries. Representative snapshots from angiograms of all RVGs and SVGs in animals that survived to 12 months are shown in **Figure 4** (snapshots in all animals are shown in Supplemental Figure 3).

QCA (**Table 1,** Supplemental Tables 1 and 2, **Figures 5 and 6**) showed that RVGs had geometric stable reference diameters at baseline (3.76 ± 0.84 mm; n = 8), 1 month (3.59 ± 0.31 mm; n = 11), 3 months (3.54 ± 0.48 mm; n = 10), 6 months (3.46 ± 0.32 mm; n = 9), 9 months (2.94 ± 0.22; N = 6), and 12 months (3.29 ± 0.33 mm; n = 5). SVG reference diameter showed progressive diffuse dilatation at baseline (4.29 mm; n = 1), 1 month (5.82 ± 0.55 mm; n = 3), 3 months (7.37 ± 1.61 mm; n = 3), 6 months (8.56 ± 2.29 mm; n = 3) and 12 months (9.47 ± 1.88 mm; n = 3) as shown in **Figures 5A and 6**. RVG minimum lumen diameter decreased from 1 month (2.67 ± 0.30 mm; n = 11) to 3 months (2.13 ± 0.40 mm; n = 10) and remained stable thereafter: 6 months (2.13 ± 0.40 mm; n = 9), 9 months (1.93 ± 0.46; n = 6), and 12 months (2.24 ± 0.46 mm; n = 5). SVG minimum lumen diameter progressively increased: 1 month (2.81 ± 0.72 mm; n = 3), 3 months (3.96± 1.69 mm; n = 3), 6 months (3.78 ± 0.93 mm; n = 3), and 12 months (4.69 ± 0.66 mm; n = 3) (**Figures 5B and 6, Table 1**).

Figures 5B and 6 show that between 1 and 3 months, in the RVGs, the flow velocity increased (mean 7.9 to 14.9 cm/s); thereafter, there were no

FIGURE 5 **Serial Plots of Angiographic Parameters for All Animals**

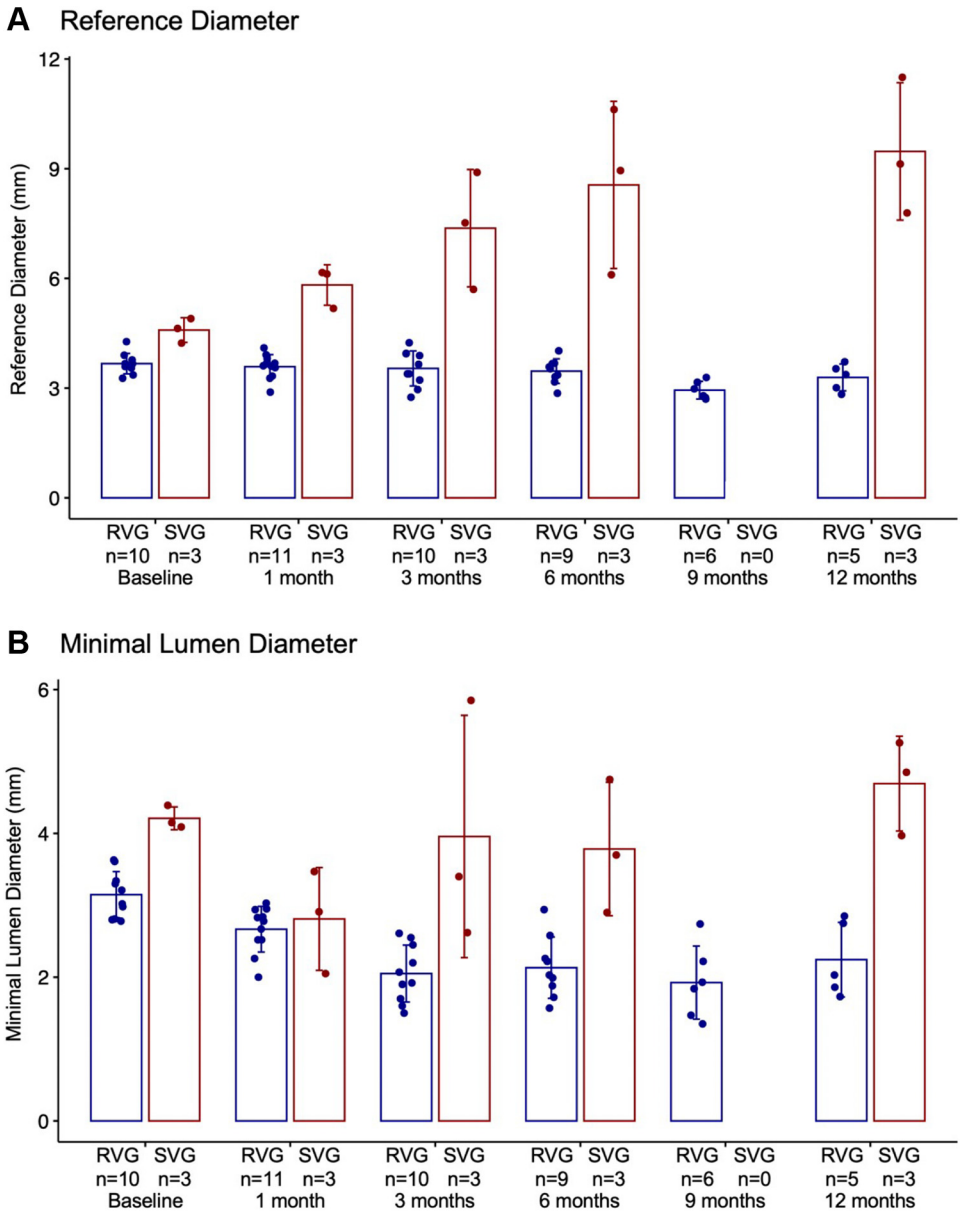

Serial changes of reference diameter **(A)**, minimal lumen diameter **(B)**, flow speed **(C)**, and quantitative flow ratio (QFR) **(D)** in both RVGs **(blue)** and SVGs **(red)**. **Bars** are the SD of the mean. One occluded RVG (restorative vascular graft) (3-month follow-up) was not included in the graphs (19S0204).

Continued on the next page

significant changes in flow velocity. Figures 5B and 6 also show that flow velocities remained low (2.3 cm/s at 1 month and 3.4 cm/s at 12 months) in the SVGs.

At 1 month, QFR was not analyzable in 4 cases (2 in RVG, 2 in SVG) due to lack of isocenter calibration or because of a poor angiographic image quality. Figures 5D and 6 present the QFR values for both RVGs and SVGs. Despite the lower flow speed in the SVGs compared with the RVGs, the QFR values are similar for both. Figure 7 displays one representative case of an RVG and SVG, respectively, with serial QFR follow-ups out to 12 months. Between 1 month and 3 months, there was a significant decrease in QFR for the RVGs (n = 10) (mean: 0.98 to 0.78). From

FIGURE 5 Continued

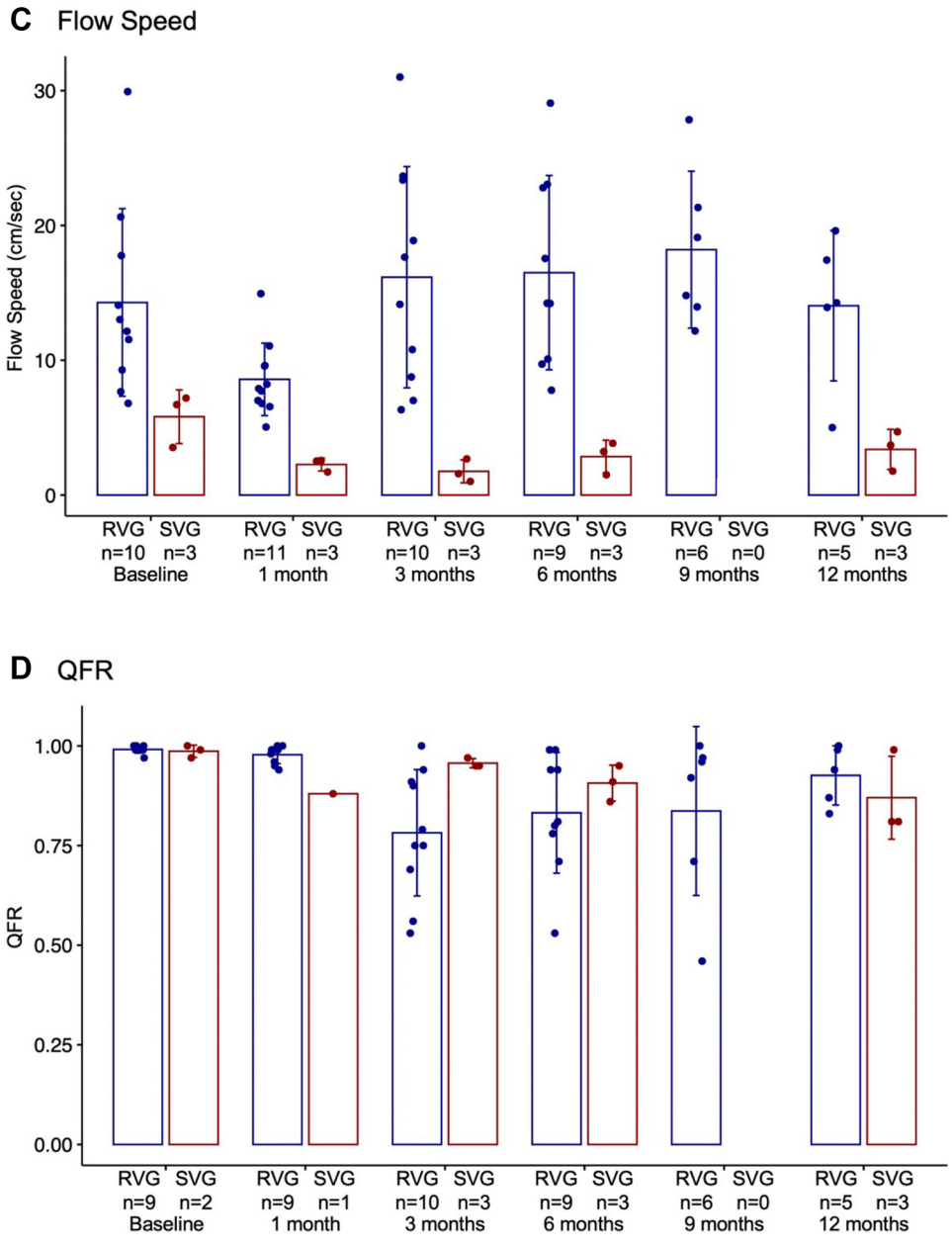

3 months (n = 10) to 12 months (n = 5), the QFR in the RVGs exhibited an increasing or stable trend up to 12 months (QFR: 0.93). In the SVGs, none of the QFR measurements was below 0.80.

DISCUSSION

The present study was an investigation of an electrospun, polymeric, restorative graft intended for coronary artery bypass surgery as an alternative to SVGs. We observed that the device exhibited adequate patency and superior flow and diametrical uniformity, compared with SVG controls, in an ovine CABG model with survival to 1 year. There were animal model-related complications that resulted in animals being implanted but did not survive, which required them to be replaced with additional backup animals. There were other animal model complications that resulted in animals being euthanized before their intended time points.

FIGURE 6 **Series of All Measurements for Each Angiography-Derived Parameter Over Follow-Up Period**

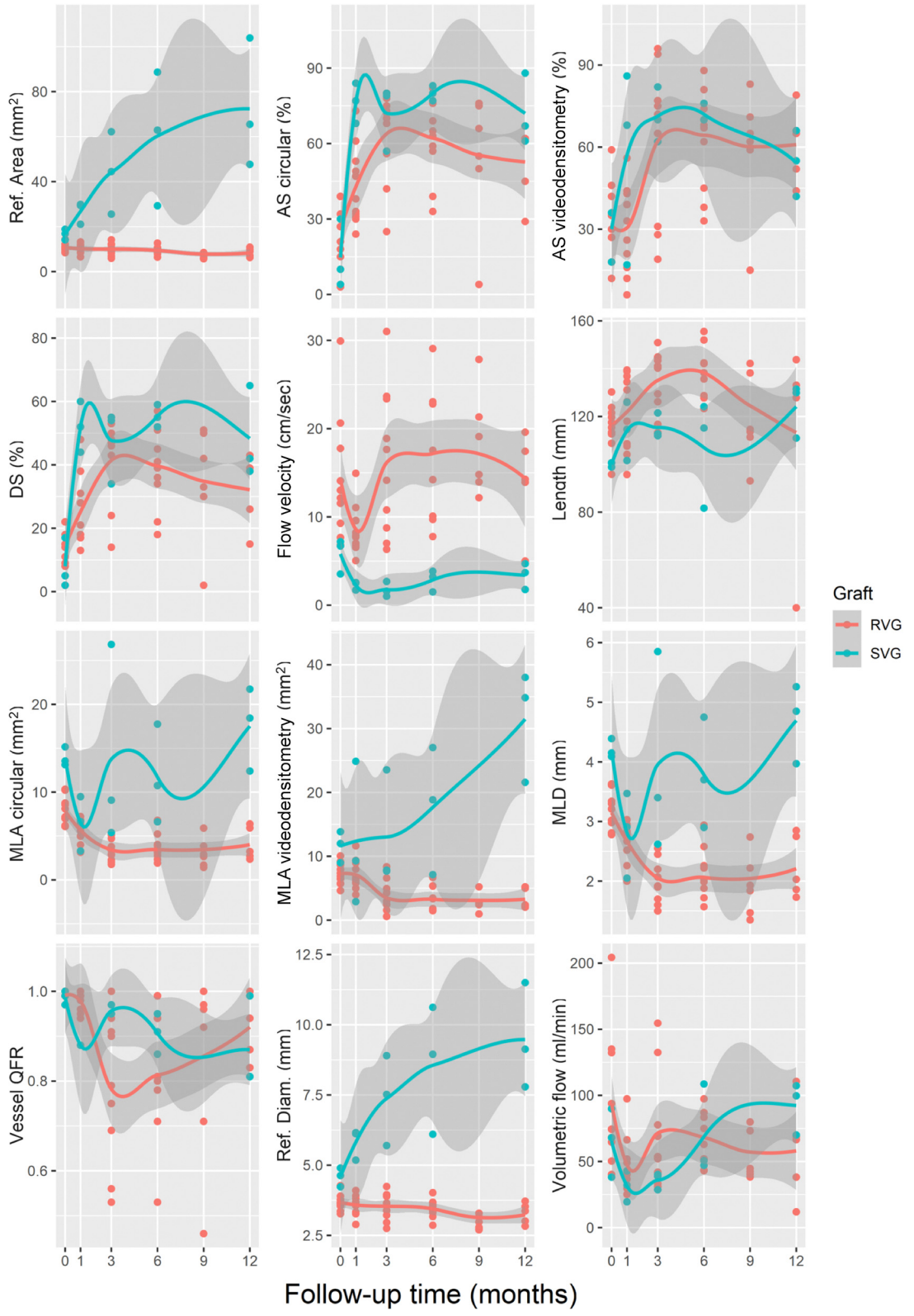

Measurements are color-coded by group (RVG and SVG) with a smoothed average (locally estimated scatterplot smoothing) over time plotted for each group to illustrate group differences and changes over time. AS = area stenosis; DS = diameter stenosis; MLA = minimum lumen area; MLD = minimum lumen diameter; Ref. Diam. = reference diameter. Abbreviations as in Figures 3 and 5.

FIGURE 7 Representative Examples of Serial QFR in Cases of RVG and SVG

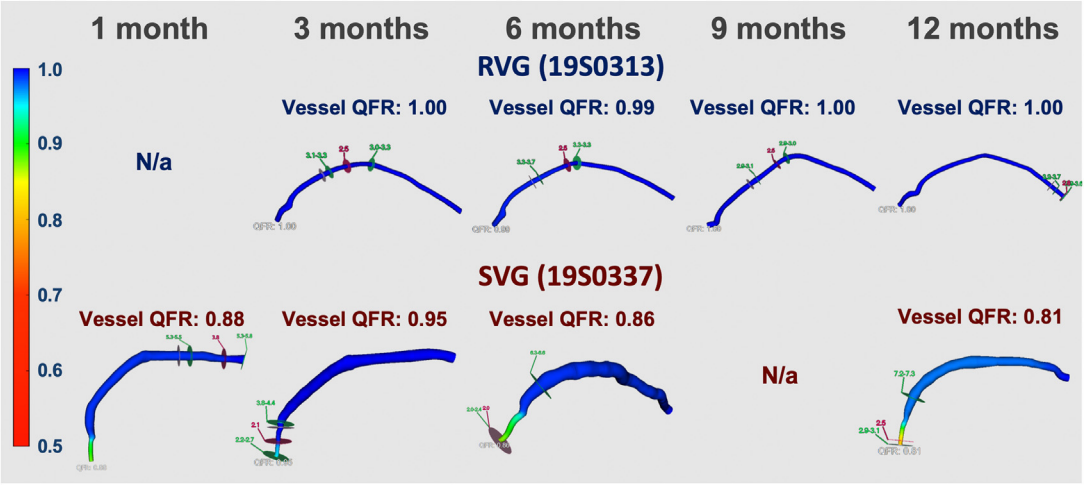

This figure shows one representative case of an RVG and SVG, respectively, with serial QFR follow-ups out to 12 months. Abbreviations as in Figures 3 and 5.

The ovine CABG model is challenging, which is exemplified by scarcity of scientific literature, especially on synthetic graft evaluation.[41,42] The only paper identified on 12 months of follow-up with a synthetic graft lacked important metrics on study design, which makes it difficult to judge on its merits.[43] Even with less challenging arterial bypass models (carotid interposition, femoral-femoral, or iliac-femoral), and relatively short graft lengths (typically 5-7 cm), patency on small-diameter synthetic grafts (≤4 mm internal diameter) has been reported between 0% and 25% in studies extending beyond 1 month of follow-up.[41] Saphenous vein grafting for CABG has been reported in literature for sheep[44,45] and baboon.[46] Reported patency and dilation of SVGs appears to be in line with the present study findings. In this light, the aggregated patency at 6 months' follow-up of 91% (10 of 11) in the present study for the RVG, especially given implant length (~15 cm) and location, was considered a very promising result. Besides 1 occlusion, only 1 animal was euthanized before the 6-month follow-up with an apparent distal stenosis in the RVG. Autopsy revealed a luminal protrusion of the implant material at the distal anastomosis as a result of suboptimal suture placement as the most likely nidus for the neointima formation, resulting in the observed stenosis. Of the 2 animals that were euthanized at the 6-month follow-up, one had a graft aneurysm shown on angiography, which was later confirmed by histopathology. It was postulated that it could be related to local high curvature and dynamic bending along the graft trajectory, likely due to the specifics of the animal model (grafting from the descending aorta to the LAD and bending around the pulmonary artery). A more detailed analysis of the impact of mechanical factors (ie, bending angle, superficial wall strain, minimum and maximum endothelial shear stress) at baseline on late flow metrics of the grafts has been published separately.[47] The other 6-month explant had revealed neointimal delamination during the 6-month OCT follow-up, which was suggested to be due to an interaction between the catheter and locally high graft curvature (Supplemental Figure 2). This graft was patent at euthanasia. Although this cautions the use of OCT in tortuous segments in the early remodeling, it should be noted that the tortuosity is considered a feature of the preclinical model and could be avoided clinically with careful case planning.

Based on positive angiographic assessment of the remaining RVGs (n = 7) and SVGs (n = 3) at 6 months' follow-up, it was decided to extend the study to an exploratory 12-month endpoint, to maximize learning. During this exploratory phase, 2 unscheduled deaths for the RVG animals were noted. One was shortly before the 9-month angiography; autopsy revealed a recanalized thrombus in the distal graft, shortly distal to a mild stenosis observed at the 6-month angiography. The other at 10 months'

FIGURE 8 Micro-CT Profile and Histologies at 12 Months

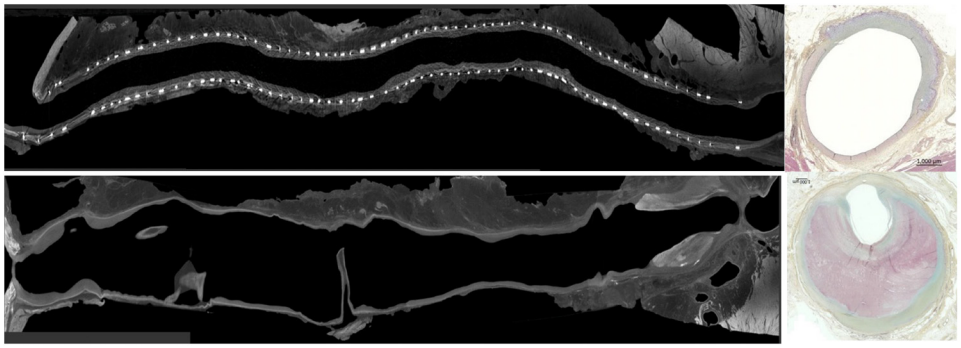

Micro-computed tomography (CT) profile at 12-month explant of RVG **(upper left)** and SVG **(lower left)**. **(Right)** Histology cross-sections near distal anastomosis of each graft (**upper right**, RVG; **lower right**, SVG). Abbreviations as in **Figures 3 and 5**.

follow-up revealed a mid-graft occlusion, co-locating with an area of potential neointima denudation during the intravascular imaging performed at 6 months' follow-up. Of note, distal and proximal anastomoses in both grafts were widely patent.

A critically important result of this study was that 5 of 7 RVGs remained patent out to 1 year follow-up, thus pushing the frontier on preclinical evaluation of small-diameter grafts in a preclinical CABG model. Although the SVGs also remained patent, it is believed that this finding is partly attributable to their progressive diffuse dilation. Micro-computed tomography analysis of SVG 12-month explants confirmed a nonuniform dilated lumen, with indications of neointimal tissue build-up near the distal anastomosis. Histopathology confirms similarity to the clinical disease process that has been described for SVGs, which eventually leads to distal anastomotic IH and eventual occlusion.[1] RVG 12-month explant micro-computed tomography and histopathology in contrast shows a more uniform lumen with no apparent changes at the anastomoses (**Figure 8**). It is suggested from the level of distal anastomosis IH seen in the SVGs in this study that a progressive pathologic process is ongoing that could ultimately cause occlusions, which is in line with both preclinical and clinical evidence.[41,48] Quantitative angiography revealed that RVGs maintained an overall uniform and nondilating lumen throughout the duration of the study. This is in stark contrast to the SVGs in this study, and as also reported in previous work, which showed that SVGs exhibited progressively increasing dilation over time, doubling the initial diameter by 1 year.[31] A uniform diameter has been proposed to be a key factor in mitigating IH development by maintaining a uniform shear stress on the graft lumen.[13,49,50] **Figures 5 and 6** and Supplemental Table 2 present a comparison between an RVG and an SVG implanted for 1 year as an ovine CABG. The near doubling in diameter of the SVG relative to the RVG is noteworthy. Also worth noting is the dramatic increase in neointima formation in the distal anastomosis of the SVG compared with the stable neointima in the RVG. Although there was an initial period between 1 and 3 months when the RVG minimal lumen diameter decreased and consequently so did the QFR, there appeared to be a stable or increasing trend in MLD and QFR over time. This mechanism is under further investigation and will be the subject matter of future reports.

Finally, RVGs that can maintain a controlled, uniform diameter could allow for improved size matching to the target artery and reduced flow disturbances, which could further attenuate IH.[51-53] Diameter matching has also been reported to accelerate in vivo re-endothelialization in arteries and vascular grafts.[54,55] Thus, by preventing dilation, maintaining diameter uniformity, and improving diameter matching of the CABG (4 mm) to the target coronary artery (2 mm), the RVG maintained improved hemodynamics compared with SVG controls in this ovine model out to 1 year.

STUDY LIMITATIONS. We acknowledge that our study has several limitations. First, the current study was conducted in a limited sample size (XABG: N = 13, SVG: N = 3) and during a follow-up period of 12 months. The restorative process following the

biodegradation of the polymer may take longer; therefore, late dynamic change of the graft may occur beyond 12 months.

Second, ovine with adverse findings such as aneurysmal or thrombotic change were euthanized shortly after the disclosure of these findings, in agreement with the advisory board. Therefore, the surviving cases might be biased towards good (or bad) outcomes especially in the late phases of the follow-up (6-12 months).

Third, the lumen and flow measurements at each time point were evaluated based on angiography without pressure- and velocity-wire insertion. Therefore, the various parameters derived from the angiography are highly dependent on the quality of angiography and were not validated with other modalities. There was only incidental use of optical coherence tomography.

Finally, the present study is a preclinical study with ovine model. The remodeling response following implantation of grafts and late results may be different in other animal species and in human beings.

CONCLUSIONS

The ovine CABG model proved to be a demanding experimental set-up; however, it was a rigorous approach to prepare for clinical translation of this novel technology. The serial angiographic assessment of the RVGs in this study provided important data for the safety of the device, which will help to enable this clinical translation.

ACKNOWLEDGEMENTS The authors thank the team at American Preclinical Services.

FUNDING SUPPORT AND AUTHOR DISCLOSURES

The work described in this paper was fully funded by Xeltis BV. Drs El-Kurdi, Reinöhl, and Cox are all employees of Xeltis. Dr Virmani has received personal fees from Xeltis, and Medtronic; as well as Institutional grants from Abbott Vascular, Boston Scientific, Medtronic, Xeltis and Becton Dickinson. Prof. Onuma has received institutional research grants related to his work as the Chairman of cardiovascular imaging core labs of several clinical trials and registries sponsored by industry, for which he receives no direct compensation. Prof. Serruys has received personal fees from Sino Medical Sciences Technology, Philips/Volcano and Xeltis. All other authors have reported that they have no relationships relevant to the contents of this paper to disclose.

ADDRESS FOR CORRESPONDENCE: Dr Patrick W. Serruys, National University of Ireland, Galway (NUIG), University Road, Galway H91 TK33, Ireland. E-mail: patrick.w.j.c.serruys@gmail.com.

PERSPECTIVES

COMPETENCY IN MEDICAL KNOWLEDGE: Many attempts have been made to inhibit or counteract SVG failure modes; however, only external support for SVGs has gained momentum in clinical utility. This study revealed the feasibility of implantation, and showed good patency out to 12 months of the novel bio-restorative grafts, in a challenging ovine CABG model.

TRANSLATIONAL OUTLOOK: This finding could trigger the first-in-man trial of using the novel material instead of SVG. We believe that eventually, this novel biorestorative bypass graft can be one of the options for CABG patients who have difficulty harvesting SVG.

REFERENCES

1. Taggart DP, Ben Gal Y, Lees B, et al. A randomized trial of external stenting for saphenous vein grafts in coronary artery bypass grafting. *Ann Thorac Surg*. 2015;99:2039–2045.

2. Mack MJ, Squiers JJ, Lytle BW, DiMaio JM, Mohr FW. Myocardial revascularization surgery: JACC historical breakthroughs in perspective. *J Am Coll Cardiol*. 2021;78:365–383.

3. Lytle BW, Blackstone EH, Sabik JF, Houghtaling P, Loop FD, Cosgrove DM. The effect of bilateral internal thoracic artery grafting on survival during 20 postoperative years. *Ann Thorac Surg*. 2004;78:2005–2012 [discussion 2012-2014].

4. Ghista DN, Kabinejadian F. Coronary artery bypass grafting hemodynamics and anastomosis design: a biomedical engineering review. *Biomed Eng Online*. 2013;12:129.

5. Ojha M, Cobbold RS, Johnston KW. Influence of angle on wall shear stress distribution for an end-to-side anastomosis. *J Vasc Surg*. 1994;19:1067–1073.

6. Sottiurai VS. Distal anastomotic intimal hyperplasia: histocytomorphology, pathophysiology, etiology, and prevention. *Int J Angiol*. 1999;8:1–10.

7. Alexander JH, Ferguson TB Jr, Joseph DM, et al. The PRoject of Ex-vivo Vein graft ENgineering via Transfection IV (PREVENT IV) trial: study rationale, design, and baseline patient characteristics. *Am Heart J*. 2005;150:643–649.

8. Fitzgibbon GM, Kafka HP, Leach AJ, Keon WJ, Hooper GD, Burton JR. Coronary bypass graft fate and patient outcome: angiographic follow-up of 5,065 grafts related to survival and reoperation in 1,388 patients during 25 years. *J Am Coll Cardiol*. 1996;28:616–626.

9. Yun KL, Wu Y, Aharonian V, et al. Randomized trial of endoscopic versus open vein harvest for coronary artery bypass grafting: six-month patency rates. *J Thorac Cardiovasc Surg*. 2005;129:496–503.

10. Shears LL 2nd, Kibbe MR, Murdock AD, et al. Efficient inhibition of intimal hyperplasia by adenovirus-mediated inducible nitric oxide synthase gene transfer to rats and pigs in vivo. *J Am Coll Surg*. 1998;187:295–306.

11. Petrofski JA, Hata JA, Gehrig TR, et al. Gene delivery to aortocoronary saphenous vein grafts in a large animal model of intimal hyperplasia. *J Thorac Cardiovasc Surg*. 2004;127:27–33.

12. Kohler TR, Toleikis PM, Gravett DM, Avelar RL. Inhibition of neointimal hyperplasia in a sheep model of dialysis access failure with the bioabsorbable Vascular Wrap paclitaxel-eluting mesh. *J Vasc Surg*. 2007;45:1029–1037 [discussion 1037-1038].

13. Zilla P, Human P, Wolf M, et al. Constrictive external nitinol meshes inhibit vein graft intimal hyperplasia in nonhuman primates. *J Thorac Cardiovasc Surg*. 2008;136:717–725.

14. Zurbrugg HR, Wied M, Angelini GD, Hetzer R. Reduction of intimal and medial thickening in sheathed vein grafts. *Ann Thorac Surg*. 1999;68:79–83.

15. El-Kurdi MS, Hong Y, Stankus JJ, Soletti L, Wagner WR, Vorp DA. Transient elastic support for vein grafts using a constricting microfibrillar polymer wrap. *Biomaterials*. 2008;29:3213–3220.

16. El-Kurdi M, Soletti L, McGrath J, et al. Functional remodeling of an electrospun polydimethylsiloxane-based polyether urethane external vein graft support device in an ovine model. *J Biomed Mater Res A*. 2019;107:2135–2149.

17. Liu SQ, Moore MM, Glucksberg MR, Mockros LF, Grotberg JB, Mok AP. Partial prevention of monocyte and granulocyte activation in experimental vein grafts by using a biomechanical engineering approach. *J Biomech*. 1999;32:1165–1175.

18. Emery R, Solien E, Puskas J. Saphenous vein graft wrapping by nitinol mesh: a word of caution. *Thorac Cardiovasc Surg*. 2015;63:298–299.

19. Rescigno G, Aratari C, Matteucci SM, et al. Saphenous vein graft wrapping by nitinol mesh: a word of caution. *Thorac Cardiovasc Surg*. 2015;63:292–297.

20. Belczak CE, Tyszka AL, Godoy JM, Ramos RN, Belczak SQ, Caffaro RA. Clinical complications of limb undergone harvesting of great saphenous vein for coronary artery bypass grafting using bridge technique. *Rev Bras Cir Cardiovasc*. 2009;24:68–72.

21. Nicolini F. Editorial on the article entitled "Secondary surgical-site infection after coronary artery bypass grafting: a multi-institutional prospective cohort study. *J Thorac Dis*. 2018;10:S3938–S3941.

22. Sapsford RN, Oakley GD, Talbot S. Early and late patency of expanded polytetrafluoroethylene vascular grafts in aorta-coronary bypass. *J Thorac Cardiovasc Surg*. 1981;81:860–864.

23. Laube HR, Duwe J, Rutsch W, Konertz W. Clinical experience with autologous endothelial cell-seeded polytetrafluoroethylene coronary artery bypass grafts. *J Thorac Cardiovasc Surg*. 2000;120:134–141.

24. Dohmen PM, Pruss A, Koch C, Borges AC, Konertz W. Six years of clinical follow-up with endothelial cell-seeded small-diameter vascular grafts during coronary bypass surgery. *J Tissue Eng*. 2013;4:2041731413504777.

25. Emery RW, Mills NL, Teijeira FJ, et al. North American experience with the Perma-Flow prosthetic coronary graft. *Ann Thorac Surg*. 1996;62:691–695 [discussion 695-696].

26. Weyand M, Kerber S, Schmid C, Rolf N, Scheld HH. Coronary artery bypass grafting with an expanded polytetrafluoroethylene graft. *Ann Thorac Surg*. 1999;67:1240–1244 [discussion 1244-1245].

27. Zilla P, Bezuidenhout D, Human P. Prosthetic vascular grafts: wrong models, wrong questions and no healing. *Biomaterials*. 2007;28:5009–5027.

28. Pennel T, Zilla P, Bezuidenhout D. Differentiating transmural from transanastomotic prosthetic graft endothelialization through an isolation loop-graft model. *J Vasc Surg*. 2013;58:1053–1061.

29. Taylor G. Disintegration of water drops in electric field. *Proc R Soc London Ser A*. 1964;280:383–397.

30. Shofti R, Zaretzki A, Cohen E, Engel A, Bar-El Y. The sheep as a model for coronary artery bypass surgery. *Lab Anim*. 2004;38:149–157.

31. El-Kurdi MS, Soletti L, Nieponice A, et al. Ovine femoral artery bypass grafting using saphenous vein: a new model. *J Surg Res*. 2015;193:458–469.

32. Keane D, Haase J, Slager CJ, et al. Comparative validation of quantitative coronary angiography systems. Results and implications from a multicenter study using a standardized approach. *Circulation*. 1995;91:2174–2183.

33. Ozaki Y, Violaris AG, Kobayashi T, et al. Comparison of coronary luminal quantification obtained from intracoronary ultrasound and both geometric and videodensitometric quantitative angiography before and after balloon angioplasty and directional atherectomy. *Circulation*. 1997;96:491–499.

34. Kawsara A, Núñez Gil IJ, Alqahtani F, Moreland J, Rihal CS, Alkhouli M. Management of coronary artery aneurysms. *J Am Coll Cardiol Intv*. 2018;11:1211–1223.

35. Ahmad M, Mungee S. *Coronary Ectasia*. StatPearls Publishing; 2022.

36. Gibson CM, Cannon CP, Daley WL, et al. TIMI frame count: a quantitative method of assessing coronary artery flow. *Circulation*. 1996;93:879–888.

37. Meirson T, Orion E, Di Mario C, et al. Flow patterns in externally stented saphenous vein grafts and development of intimal hyperplasia. *J Thorac Cardiovasc Surg*. 2015;150:871–878.

38. Tu S, Ding D, Chang Y, Li C, Wijns W, Xu B. Diagnostic accuracy of quantitative flow ratio for assessment of coronary stenosis significance from a single angiographic view: a novel method based on bifurcation fractal law. *Catheter Cardiovasc Interv*. 2021;97(suppl 2):1040–1047.

39. Xu B, Tu S, Qiao S, et al. Diagnostic accuracy of angiography-based quantitative flow ratio measurements for online assessment of coronary stenosis. *J Am Coll Cardiol*. 2017;70:3077–3087.

40. ISO 7198:2016. Cardiovascular Implants and Extracorporeal Systems—Vascular Prostheses—Tubular Vascular Grafts and Vascular Patches, 2nd ed., International Organization for Standardization,Switzerland 2016.

41. Fang S, Ellman DG, Andersen DC. Review: tissue engineering of small-diameter vascular grafts and their in vivo evaluation in large animals and humans. *Cells*. 2021;10:713.

42. Byrom MJ, Bannon PG, White GH, Ng MK. Animal models for the assessment of novel vascular conduits. *J Vasc Surg*. 2010;52:176–195.

43. Farrar DJ. Development of a prosthetic coronary artery bypass graft. *Heart Surg Forum*. 2000;3:36–40.

44. Abbasi K, Shalileh K, Anvari MS, et al. Perivascular nitric oxide delivery to saphenous vein grafts prevents graft stenosis after coronary artery bypass grafting: a novel sheep model. *Cardiology*. 2011;118:8–15.

45. Ben-Gal Y, Taggart DP, Williams MR, et al. Expandable external support device to improve saphenous vein graft patency after CABG. *J Cardiothorac Surg*. 2013;8:122.

46. Moodley L, Franz T, Human P, et al. Protective constriction of coronary vein grafts with knitted nitinol. *Eur J Cardiothorac Surg*. 2013;44:64–71.

47. Wu X, Ono M, Poon EKW, et al. One-year performance of biorestorative polymeric coronary bypass grafts in an ovine model: correlation between early biomechanics and late serial quantitative flow ratio. *Eur J Cardiothorac Surg*. 2022;61:1402–1411.

48. Buja LM, Schoen FJ. Chapter 14 - the pathology of cardiovascular interventions and devices for coronary artery disease, vascular disease, heart failure, and arrhythmias. In: *Buja LM, Butany J, editors. Cardiovascular Pathology (4th ed.)*. San Diego: Academic Press, 2016:577–610.

49. Min SK, Kenagy RD, Jeanette JP, Clowes AW. Effects of external wrapping and increased blood flow on atrophy of the baboon iliac artery. *J Vasc Surg*. 2008;47:1039–1047.

50. Zilla P, Moodley L, Wolf MF, et al. Knitted nitinol represents a new generation of constrictive external vein graft meshes. *J Vasc Surg*. 2011;54:1439–1450.

51. Fan L, Karino T. Effect of a disturbed flow on proliferation of the cells of a hybrid vascular graft. *Biorheology*. 2010;47:31–38.

52. Haruguchi H, Teraoka S. Intimal hyperplasia and hemodynamic factors in arterial bypass and arteriovenous grafts: a review. *J Artif Organs*. 2003;6:227–235.

53. Sunamura M, Ishibashi H, Karino T. Flow patterns and preferred sites of intimal thickening in diameter-mismatched vein graft interpositions. *Surgery*. 2007;141:764–776.

54. Cikirikcioglu M, Pektok E, Cikirikcioglu YB, et al. Matching the diameter of ePTFE bypass prosthesis with a native artery improves neoendothelialization. *Eur Surg Res*. 2008;40:333–340.

55. Vyalov S, Langille BL, Gotlieb AI. Decreased blood flow rate disrupts endothelial repair in vivo. *Am J Pathol*. 1996;149:2107–2118.

KEY WORDS coronary artery bypass graft, coronary artery disease, coronary revascularization, preclinical model, polymeric bypass graft, quantitative flow ratio, restorative vascular graft

APPENDIX For supplemental figures and a table, please see the online version of this paper.